Research paper

Exosomal miRNA confers chemo resistance via targeting Cav1/p-gp/M2-type macrophage axis in ovarian cancer

Pinar Kanlikilicer [a,b], Recep Bayraktar [a], Merve Denizli [a], Mohammed H. Rashed [a], Cristina Ivan [b,d], Burcu Aslan [a,b], Rahul Mitra [b], Kubra Karagoz [e], Emine Bayraktar [a], Xinna Zhang [b,d], Cristian Rodriguez-Aguayo [a,b], Amr Ahmed El-Arabey [a], Nermin Kahraman [a], Seyda Baydogan [a], Ozgur Ozkayar [f], Michael L. Gatza [e], Bulent Ozpolat [a,b], George A. Calin [a,b,c], Anil K. Sood [b,c,d], Gabriel Lopez-Berestein [a,b,c,∗]

[a] Department of Experimental Therapeutics, The University of Texas MD Anderson Cancer Center, Houston, Texas, USA
[b] Center for RNA Interference and Non-Coding RNA, The University of Texas MD Anderson Cancer Center, Houston, Texas, USA
[c] Department of Cancer Biology, The University of Texas MD Anderson Cancer Center, Houston, Texas, USA
[d] Department of Gynecologic Oncology and Reproductive Medicine, The University of Texas MD Anderson Cancer Center, Houston, Texas, USA
[e] Rutgers Cancer Institute of New Jersey, New Brunswick, New Jersey, USA
[f] Hacettepe University, Ankara, Turkey

ARTICLE INFO

ABSTRACT

Background: Circulating miRNAs are known to play important roles in intercellular communication. However, the effects of exosomal miRNAs on cells are not fully understood.
Methods: To investigate the role of exosomal miR-1246 in ovarian cancer (OC) microenvironment, we performed RPPA as well as many other in vitro functional assays in ovarian cancer cells (sensitive; HeyA8, Skov3ip1, A2780 and chemoresistant; HeyA8-MDR, Skov3-TR, A2780-CP20). Therapeutic effect of miR-1246 inhibitor treatment was tested in OC animal model. We showed the effect of OC exosomal miR-1246 uptake on macrophages by co-culture experiments.
Findings: Substantial expression of oncogenic miR-1246 OC exosomes was found. We showed that Cav1 gene, which is the direct target of miR-1246, is involved in the process of exosomal transfer. A significantly worse overall prognosis were found for OC patients with high miR-1246 and low Cav1 expression based on TCGA data. miR-1246 expression were significantly higher in paclitaxel-resistant OC exosomes than in their sensitive counterparts. Overexpression of Cav1 and anti-miR-1246 treatment significantly sensitized OC cells to paclitaxel. We showed that Cav1 and multi drug resistance (MDR) gene is involved in the process of exosomal transfer. Our proteomic approach also revealed that miR-1246 inhibits Cav1 and acts through PDGFβ receptor at the recipient cells to inhibit cell proliferation. miR-1246 inhibitor treatment in combination with chemotherapy led to reduced tumor burden in vivo. Finally, we demonstrated that when OC cells are co-cultured with macrophages, they are capable of transferring their oncogenic miR-1246 to M2-type macrophages, but not M0-type macrophages.
Interpretation: Our results suggest that cancer exosomes may contribute to oncogenesis by manipulating neighboring infiltrating immune cells. This study provide a new mechanistic therapeutic approach to overcome chemoresistance and tumor progression through exosomal miR-1246 in OC patients.

1. Introduction

Exosomes (nanosized vesicles) are important for communication in the tumor microenvironment (TME) [1]. They are enclosed in a lipid bilayer and are released from many types of cells, such as malignant cells, macrophages, endothelial cells and dendritic cells [2–5]. Exosomes derived from malignant tumors promote tumor proliferation, metastasis and angiogenesis by transferring their genetic information, such as messenger RNAs (mRNAs) and short non-coding microRNAs (miRNAs), to surrounding cells or distant organs.

The TME is composed by many types of cells, including, immune (e.g.monocytes and lymphocytes), and mesenchymal (e.g. fibroblasts and endothelial) cells. Malignant cells and non-transformed cells interact in the tumor microenvironment. Exosomes have been associated with tumor progression and metastasis and confer drug resistance

∗ Corresponding author at: Department of Experimental Therapeutics, 1901 East Road, Unit 1950, The University of Texas MD Anderson Cancer Center, Houston, Texas 77030, USA.
E-mail address: glopez@mdanderson.org (G. Lopez-Berestein).

Research in context

Evidence before this study

miR-1246 has been identified as a circulating non-coding RNA in different malignancies. In addition, a recent clinical study identified circulating miR-1246 as a promising clinical diagnostic biomarker for HGSOC.

Added value of this study

This manuscript highlights the key involvement of exosomes in the facilitation of acquired resistance to chemotherapy within the tumor microenvironment in ovarian cancer. We showed that Cav1 and the multi drug resistance (MDR) genes are involved in the process of exosomal transfer. We, for the first time, found a negative correlation between Cav1 expression, which is the direct target of exosomal miR-1246, and MDR resistance protein expression in ovarian cancer. We also showed that cancer exosomes may contribute to oncogenesis by manipulating neighboring infiltrating immune cells. We identified a new mechanistic therapeutic approach targeting chemo-resistance, as well as tumor progression through exosomal miR-1246 in OC cells and patients. Exosomal miR-1246 induced a tumor-promoting phenotype; cell proliferation and drug resistance. Inhibition of miR-1246 led to the concurrent inhibition of cancer signaling pathways in vivo and in vitro. This study paves the path forward for the development of exosomal miR-1246 as a biomarker in serum as a predictor of chemotherapy resistance which could improve short survival rates of ovarian cancer patients.

Implications of all the available evidence

The *standard* management of ovarian cancer is a combination of *surgical* tumor tissue debulking and chemotherapy. Although a big progress has been made in cancer treatment during the last decades, drug resistance is still critical to the development of relapses in chemotherapy-treated patients. Increasing evidence shows that microRNAs play an important role in regulating the sensitivity of cancer cells. However, the mechanism of microRNA-mediated drug resistance is not fully understood. Identification and inhibition of oncogenic circulating miR-1246 in combination with paclitaxel treatment provides a rationale approach for chemo sensitization and antitumor therapy for OC patients.

[6–8]. In fact, the role exosomes play in the tumor microenvironment drives tumor progression and metastasis. Exosomes have also been shown as the initiators of pre-metastatic niche formation in different types of cancer cells [9,10]. What really makes exosome mediated communication such an important field are the findings that exosomes contain functional mRNAs and miRNAs and the fact that these RNAs are transferrable to target cells. For instance, miRNAs in cancer exosomes are considered hormones, which hold special importance in mediating cancer metastasis [11].

miRNAs are part of a large family of non-coding RNAs that regulate many important cellular functions, such as cell signaling, cancer-related inflammation, T-cell and stem cell differentiation and metabolic homeostasis [12–16]. Circulating miRNAs have been proposed as biomarkers in many cancers [16–19]. miR-1246, a commonly reported circulating miRNA, was found to be elevated in serum samples of patients with esophageal squamous cell, small cell lung and colon, breast, cervical and ovarian cancers [18,20–24]. miR-1246 levels were also found to be higher in exosomes compared to the cell of origin levels in several cancers [20,25]. miR-1246 has many oncogenic functions, such as tumor initiation, proliferation and metastasis [24,26,27].

Recently, we demonstrated that ovarian cancer (OC) exosomes are loaded with specific miRNAs and that cancer cells use these miRNAs to modify their microenvironment by releasing them via exosomes [28,29]. Due to the fact that both oncogenic and tumor suppressor miRNAs are present in exosomes, one of the most important question yet to be answered is how cancer cells program their exosomal materials to promote tumorigenesis. In this study, we sought to investigate the role of miR-1246 which is released in excess amount to the extracellular environment through their exosomes in OC cells. We demonstrated that exosomal genetic material is taken up by infiltrating pro-tumorigenic cells present in the tumor microenvironment, which indicates that the tumor microenvironment promotes tumor progression and chemo resistance through the help of cancer exosomes.

2. Results

2.1. Exosomal miR-1246 is abundantly expressed in OC exosomes

Previously, we identified miR-1246 as the most highly upregulated miRNA in chemotherapy-sensitive (F·C ≥ +233) and -resistant (F·C ≥ +131) OC exosomes (HeyA8, HeyA8-MDR, SKOV3-ip1, SKOV3-TR, A2780, A2780-CP20) compared to the cells of origin ($p < 0.05$, t-test) in a microarray experiment [28] (Fig. 1a). In the present study, we focused on the role of miR-1246 in both OC cells and OC-derived exosomes. Exosomes were characterized by nanosight, western botting and TEM as previously shown [28,29]. We validated upregulation of miR-1246 in exosomes by qPCR using two different exosomal RNA; exosomes isolated using FBS obtained by ultracentrifuge and commercially available bovine-serum free FBS (Gibco) (Supplementary Fig. 1a). We next compared miR-1246 expression in non-transformed ovarian epithelial cell exosomes versus OC cells. We found that miR-1246 was expressed to a greater extent in OC cells compared to normal ovarian surface epithelial cells (Avg. F·C > +31), as well as in OC exosomes compared to exosomes derived from normal cells (Avg. F·C > +12) (Fig. 1b and c). We also examined the level of miR-1246 in OC patients. To this end, we evaluated miR-1246 expressions by performing qPCR on RNA samples isolated from normal ovarian vs OC tissue. Consistent with our in vitro data, OC patients had high expression of miR-1246 compared to healthy controls (Fig. 1d). Analysis of clinical data from the Cancer Genome Atlas (TCGA) including 138 samples with detectable miR-1246 expression, demonstrated that high expression of miR-1246 expression had a significantly ($p = 0.036$) worse overall prognosis compared to those patients with low, yet detectable, miR-1246 expression (Fig. 1e).

Next, we investigated whether miR-1246 and exosomes co-localized in the tumor samples obtained from OC patients. Since tetraspanins are used as exosomal markers, we used CD63 antibody to stain exosomes by in situ hybridization. miR-1246 probe (Exiqon) was used to detect miR-1246 localization in the cells. We found strong colocalization of miR-1246 within the exosomes (Fig. 1f). miR-1246 was found to be localized in the nucleus. To further confirm positive nuclear expression, we also performed in situ hybridization (ISH) using OC patient tissues (Fig. 1g). We isolated miRNAs from nuclear and cytoplasmic fractions of HeyA8 OC cells. Although strong nuclear staining for miR-1246 was observed in patient tissues, miR-1246 was found to be expressed in both the nuclear and cytoplasmic fractions of OC cells (Fig. 1h).

2.2. Cav1/PDGFRβ signaling is altered by miR-1246

To determine miR-1246 downstream protein signaling, we treated SKOV3-ip1 OC cells with miR-1246 mimics and analyzed the changes in protein levels using reverse phase protein array (RPPA). We validated increased miR-1246 levels in SKOV3 cells upon miR-1246 mimic
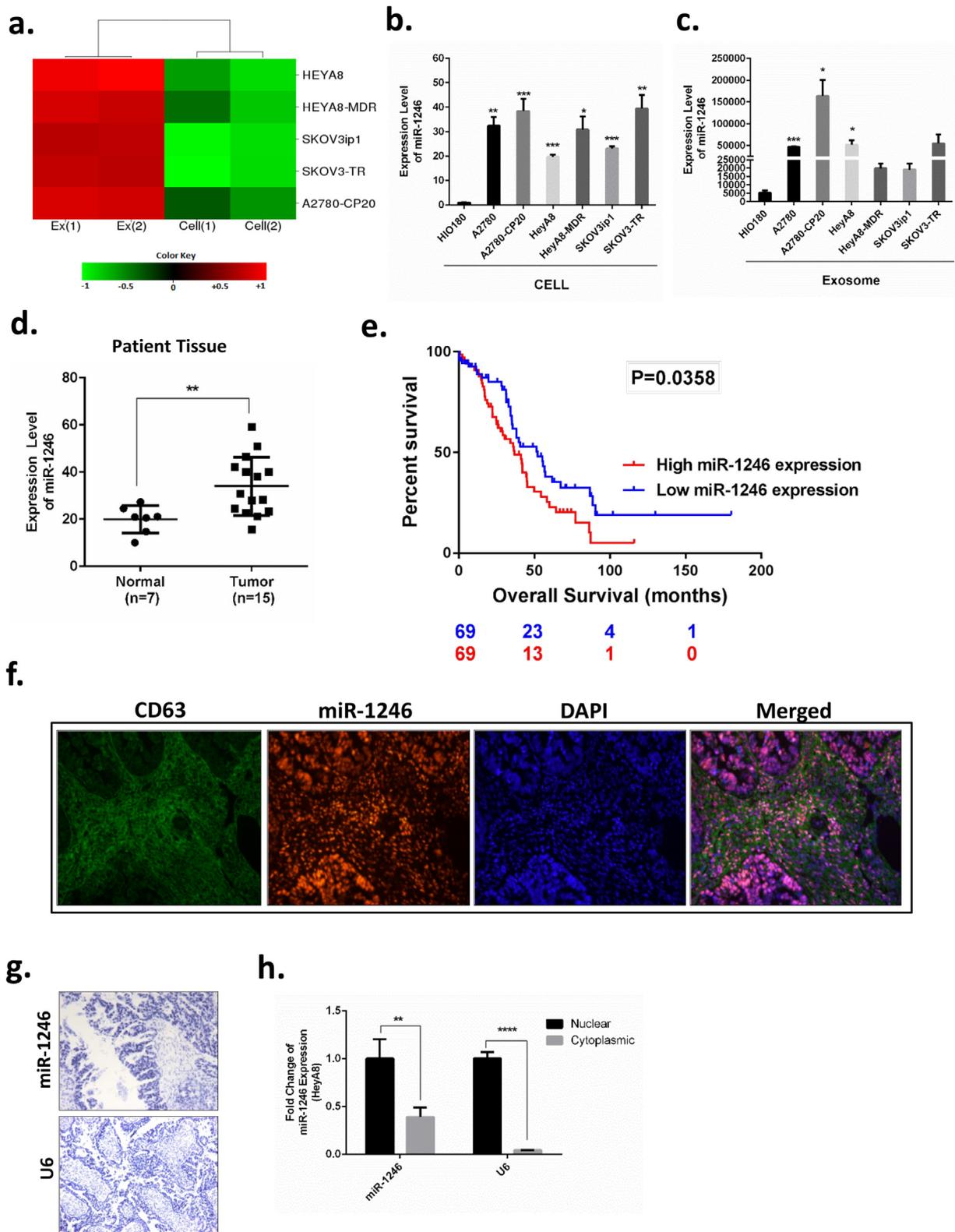
Fig. 1. Identification of exosomal miR-1246 in OC cells. a. Heat map representation of microarray results for miR-1246. The rows represent individual OC cell lines, and the columns represent the cellular localization of miR-1246 expression. Green represents downregulation; red represents upregulation. b. Comparison of miR-1246 expression in OC cells vs immortalized normal human ovarian surface epithelial cells (HIO180) by qPCR. c. Comparison of miR-1246 expression in exosomes derived from OC cells and in exosomes derived from immortalized normal human ovarian surface epithelial cells (HIO180) by qPCR. d. miR-1246 expression in normal ovarian tissues ($n = 7$) and ovarian tumors ($n = 15$) from patients. e. Overall survival curve for miR-1246 in OC patients with detectable miR-1246 expression (TCGA, $n = 138$) by comparing high ($n = 69$) versus low ($n = 69$) miR-1246 expression groups. f. Co-localization of miR-1246 with exosomes shown by in situ hybridization. CD63 was used as an exosome marker (green). miR-1246 was detected using the double-DIG-labeled miRCURY LNA microRNA-1246 probe (Exiqon) (red). Cell nucleus is stained with DAPI (blue). g. In situ hybridization of miR-1246 in OC tissue. miR-1246 has strong nuclear localization. U6 was used as an internal control. h. qPCR analysis of miR-1246 isolated from nuclear and cytoplasmic fractions of HeyA8 OC cells. miR-1246 was expressed in both fractions. $*p < 0.05$, $**p < 0.01$, $***p < 0.001$, $****p < 0.0001$ (t-test), data are presented as mean $\pm$ SD.

transfection by qPCR (Supplementary Fig. 2). Pathway analysis (Ingenuity Systems) of the RPPA data showed that many important signaling pathways, (such as PTEN signaling and molecular mechanisms of cancer (details), were significantly altered upon miR-1246 mimic transfection ($p < 0.05$, t-test, Supplementary Fig. 3 a). One of the significantly altered canonical pathways was found to be platelet-derived growth factor receptor (PDGFR) tyrosine signaling (Fig. 2a). PDGFRβ was significantly upregulated by miR-1246 mimic treatment. High expression of PDGFRβ was found to be associated with poor disease-free survival in ovarian cancer patients ($p < 0.005$, log-rank test, Supplementary Fig. 3 b). We also found a substantial decrease in the expression of caveolin-1 (Cav1), a protein that directly binds to PDGFRβ and inhibits its kinase activity [30]. We focused on Cav1 downregulation by miR-1246 since it was one of the top down-regulated candidate tumor-suppressor protein found in RPPA analysis. We confirmed the decreased levels of Cav1 expressions upon miR-1246 mimic treatment found in RPPA by Western blotting (Fig. 2b).

Consistent with these data, we determined that CAV1 levels are significantly lower in HGSOC tumors compared to normal tissue in four independent datasets: GSE18271 ($p = 7.36E-08$), GSE27651 ($p = 0.0175$), GSE38666 ($p = 1.02E-12$), GSE40595 ($p = 1.13E-14$), Supplementary Fig. 3 c). Examining data from the TCGA ($n = 138$), we determined that low Cav1 expression was associated with a worse prognosis ($p < 0.01$, log-rank test) in those high-grade serous ovarian cancer patients detectable miR-1246 expression ($p < 0.01$, log-rank test) (Fig. 2c); similar results were obtained showing patients with low Cav1 expression have a poor clinical outcome by analyzing the entire TCGA cohort ($n = 482$) irrespective of miR-1246 expression (Supplementary Fig. 4). Further analyses of these samples demonstrated a significantly worse overall prognosis ($p < 0.0005$, log-rank test) for those patients with high miR-1246 and low Cav1 expressions compared to patients with low miR-1246 and high Cav1 levels (Fig. 2d).

We next examined whether miR-1246 directly inhibits Cav1 through the 3'UTR region. Targetscan database search revealed that the Cav1 3'UTR has a binding site for miR-1246. We confirmed direct
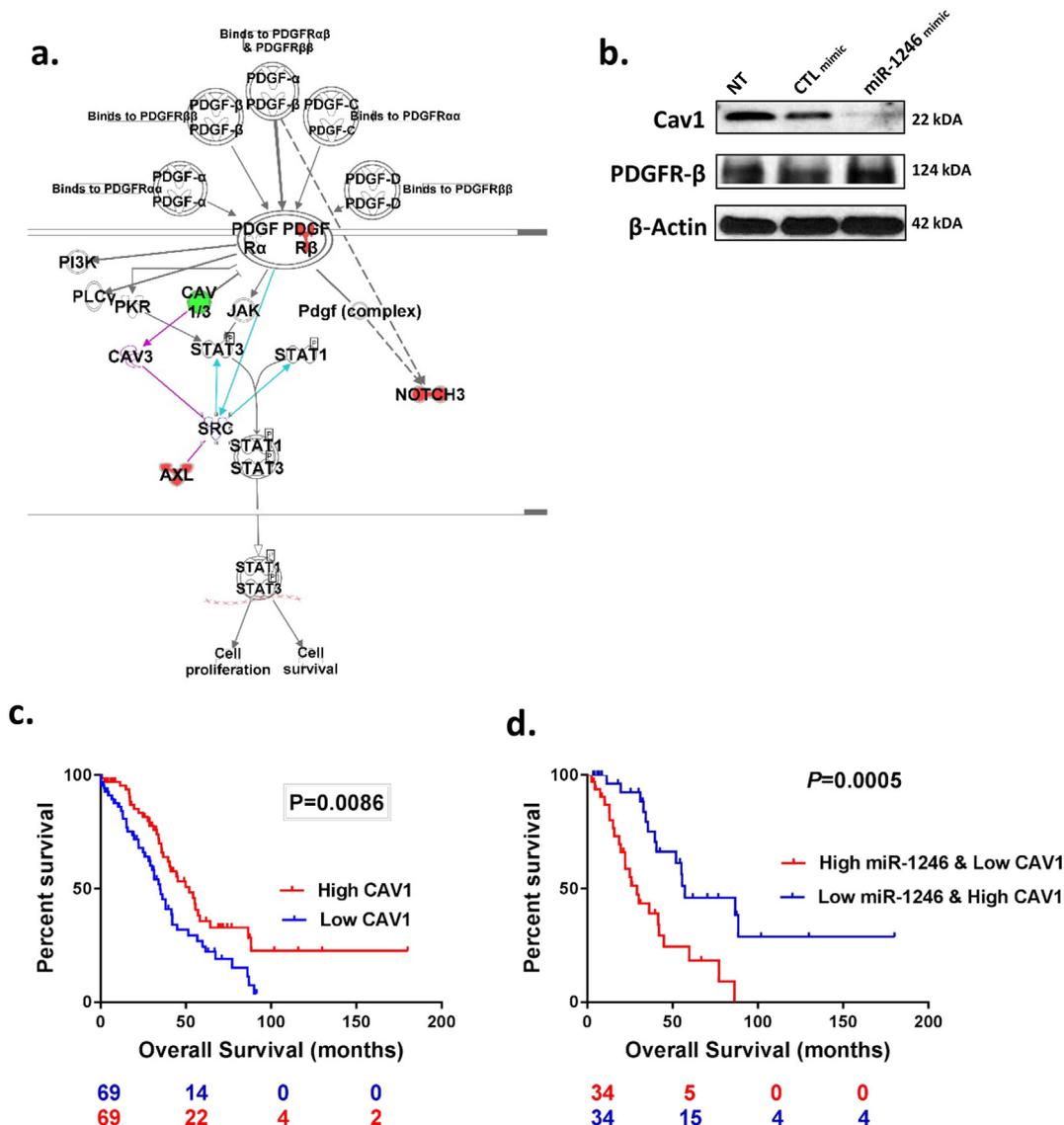
Fig. 2. Proteomic characterization of miR-1246 in OC cells. a. Ingenuity Pathway Analysis (IPA) showed that PDGFR signaling was significantly altered by miR-1246 mimic treatment. Downregulated by miR-1246 transfection in OC cells are colored green; upregulated proteins are colored red. b. Validation of Cav1 and PDGFRβ protein expression in RPPA data by western blotting in SKOV3-ip1 cells. Cells were treated with either miR-1246 or CTL miRNA for 48 h. c. Differences in overall survival curve for Cav1 in patients with detectable miR-1246 and high (n = 69) or low (n = 69) Cav1 expression. Subgroup were determined by median CAV1 expression and. Low expression level of Cav1 was associated with poor survival. d. Combination of Cav1/miR-1246 gave a better separation than Cav1 alone or miR-1246 alone for predicting overall survival.
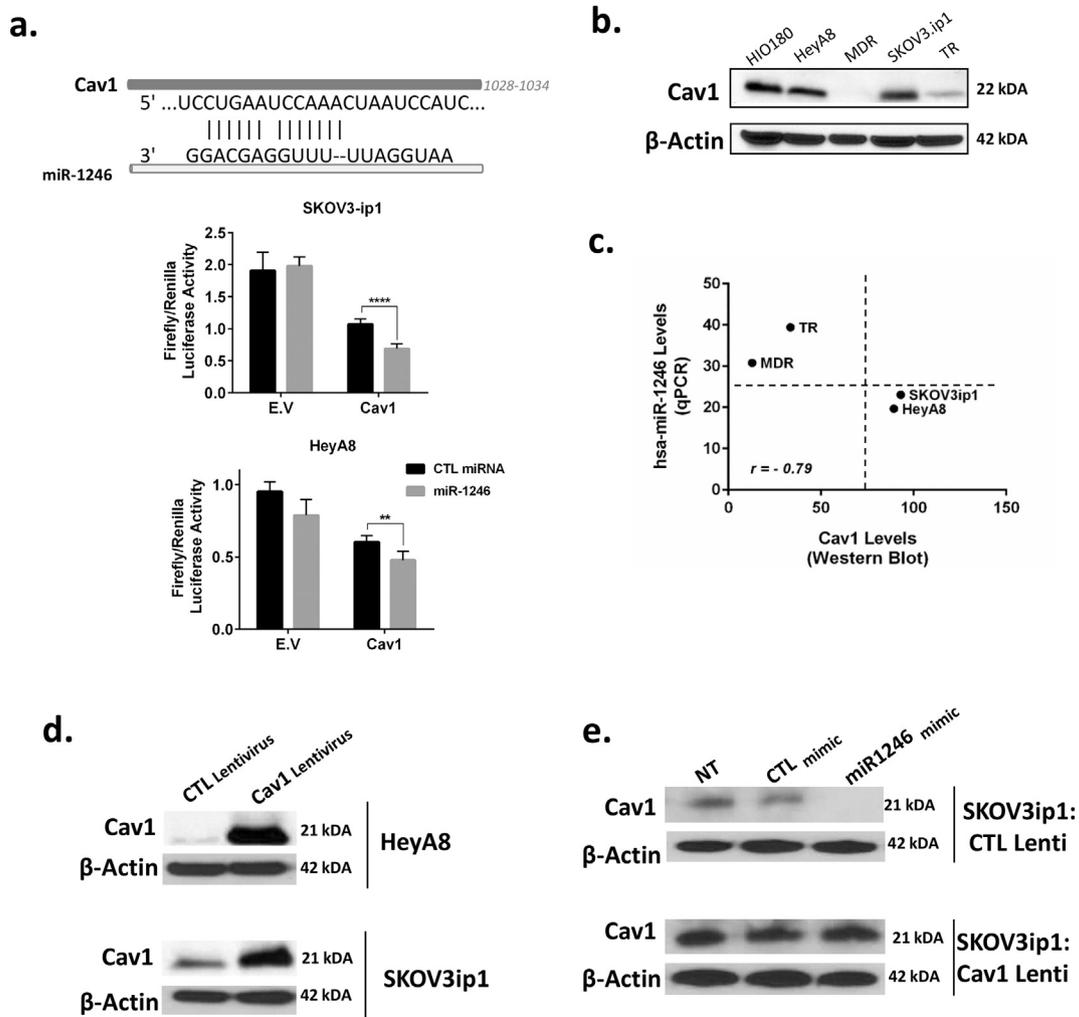
Fig. 3. Cav1 is a direct target for miR-1246. a. The sequences for the 3'UTR region of Cav1 and miR-1246. A firefly luciferase assay was used to show direct targeting of miR-1246 to Cav1. Luciferase activity in HeyA8 and SKOV3-ip1 cells co-transfected with a wild-type (WT) Cav1 transcript and with CTL miRNA mimic or miR-1246 mimic. Data were normalized to *Renilla* luciferase activity. E.V, Cav1 vector. b. Cav1 protein expression level in normal human ovarian surface epithelial cells (HIO180) and an OC panel (HeyA8, HeyA8-MDR, SKOV3-ip1, SKOV3-TR). c. A negative correlation was seen between miR-1246 level and Cav1 protein level for chemotherapy-sensitive (HeyA8, SKOV3-ip1) and -resistant OC cells (MDR, TR). Resistant and sensitive cancer cells clustered separately. d. Cav1 levels were increased using lentiviral transfection in HeyA8 and SKOV3-ip1 OC cells. e. Treatment with miR-1246 mimic decreased the levels of Cav1 in CTL lentiviral-transfected SKOV3-ip1 OC cells.

binding via a luciferase assay experiment using a pEZX-MT06 miRNA reporter vector that also contains the luciferase gene (Fig. 3a). When we co-transfected cells with pEZX-MT06, which includes the binding site for miR-1246 in the Cav1 3′-UTR, and miRNA mimics, we found around 40% and 25% inhibition in luciferase activity for the miR-1246 mimic-treated group compared to the CTL miRNA-treated group in SKOV3-ip1 and HeyA8 cells, respectively.

To determine the level of Cav1 protein expressions in different OC cells, we performed western blot experiment with four different OC cell lines together with non-transformed ovarian cells (HIO180). Interestingly, we found that Cav1 expression was lower in multidrug- and paclitaxel-resistant OC cells (HeyA8-MDR and SKOV3-TR) than in their sensitive counterparts (HeyA8 and SKOV3-ip1) (Fig. 3b). We found a strong negative correlation between miR-1246 and Cav1 expression levels in these four cell lines using the data obtained from qPCR and western blotting (Fig. 3c, $r = -0.79$). In addition, we found that drug-resistant and -sensitive OC cells clustered separately. While multidrug- and paclitaxel-resistant OC cells had high miR-1246 and low Cav1 expression, sensitive cells had low miR-1246 and high Cav1 levels (Fig. 3c).

We also performed rescue experiments using Cav1 lentiviral vector to overexpress Cav1 protein in OC cells to show that the effects on Cav1 expression are resulting from miR-1246 treatment.

Overexpression of Cav1 in HeyA8 and SKOV3-ip1 OC cells was shown by western blot (Fig. 3d). Next, we transfected SKOV3-ip1 CTL- and Cav1-lentivirus-transduced cells with either miR-1246 mimic or CTL mimic. Cav1 levels were reduced in SKOV3-ip1 cells infected by CTL lentivirus in the miR-1246-transfected group compared to the CTL miRNA-transfected group, whereas there was no difference in Cav1 expression levels among treatment groups in cells transduced with Cav1 lentivirus (Fig. 3e).

We also investigated whether silencing Cav1 using siRNA would produce similar effects on PDGFRβ expression as we obtained with miR-1246 mimic treatment. Cav1 siRNA treatment resulted in >80% inhibition of Cav1 in both SKOV3-ip1 and HeyA8 OC cells (Supplementary Fig. 5 c). PDGFRβ levels increased upon treatment with Cav1 siRNA compared to CTL siRNA (Supplementary Fig. 5 d). These results confirmed that increased PDGFRβ levels upon miR-1246 treatment are regulated through Cav1 inhibition.

2.3. miR-1246 inhibitor + chemotherapy combination reduces tumor weight in vivo

To further understand the role of miR-1246 in OC, we assessed the therapeutic efficacy of anti-miR-1246 in an intraperitoneal orthotopic SKOV3-ip1 model of OC in female athymic nude mice. To this end,
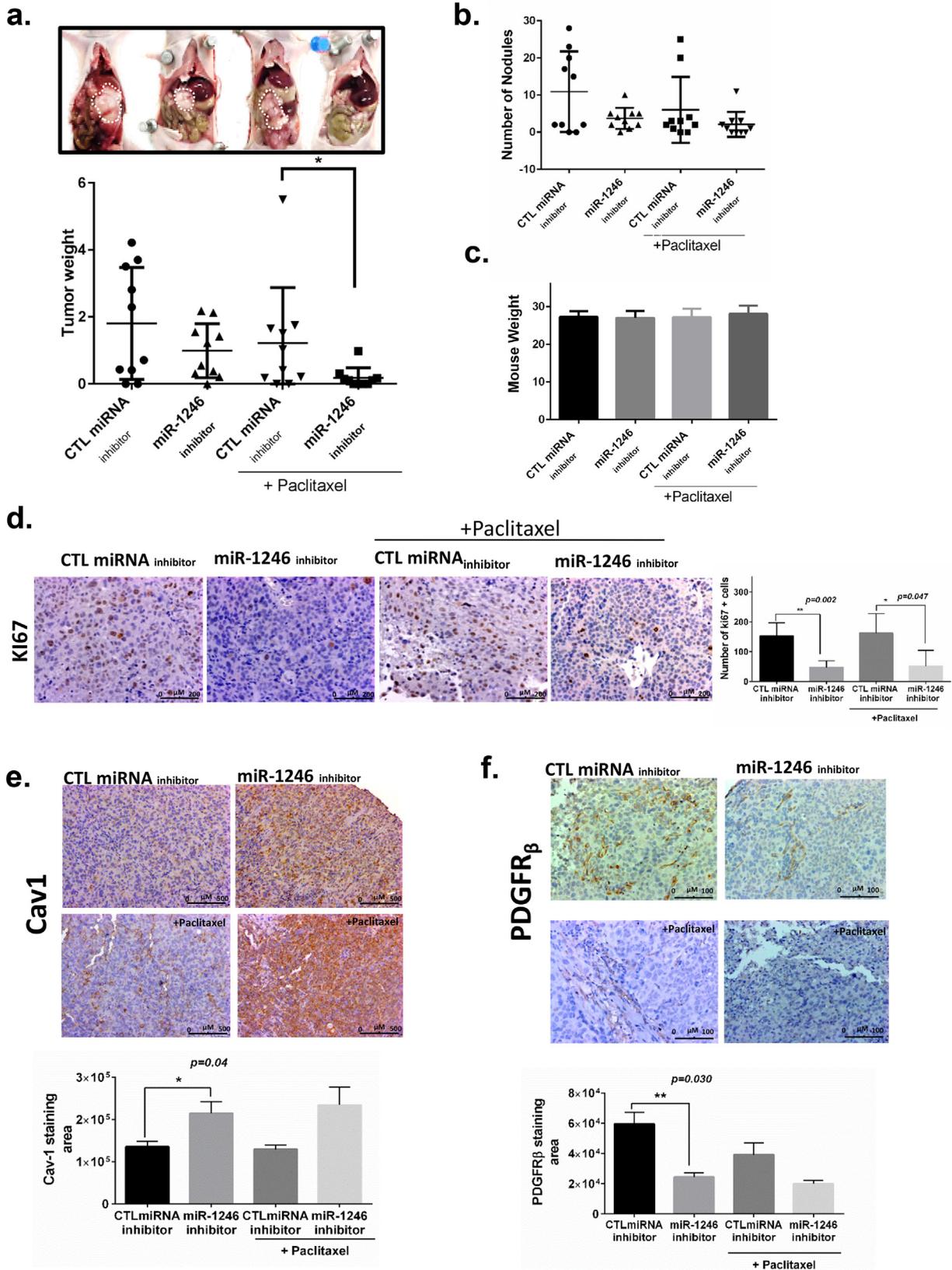
Fig. 4. miR-1246 inhibitor in combination with paclitaxel greatly reduced tumor growth in a SKOV3-ip1 mouse model.a. (Top) Comparison of the tumors obtained from representative mice treated with CTL miRNA inhibitor or miR-1246 inhibitor in DOPC particles as well as groups treated with each inhibitor in combination with paclitaxel. (Bottom) Tumor weights for groups treated with CTL miRNA inhibitor or miR-1246 inhibitor in combination with paclitaxel were significantly different ($p < 0.05$). b. There was a decreasing pattern in number of nodules in mice treated with CTL miRNA inhibitor vs miR-1246 inhibitor and with each inhibitor in combination with paclitaxel (p = n.s.). c. Mouse body weights show that there was no toxicity issue for any of the groups at the end of the treatment period. d. Immunohistochemical staining for a marker of proliferating cells (Ki67). e, f. Cav1 (e) and PDGFRβ (f) expression in tumors from mice treated with CTL miRNA inhibitor, miR-1246 inhibitor, or either inhibitor combined with paclitaxel. *$p < 0.05$, ** $p < 0.005$ (t-test), data are presented as mean ± SD.

SKOV3-ip1 cells (1×10^6 cells/200 μL Hanks balanced salt solution) were administered intraperitoneally into female nude mice to induce tumors, and 1 week later they were randomly assigned to four different treatment groups ($n = 10$). Mice were treated with miR-1246 inhibitor and CTL miRNA inhibitor alone and in combination with paclitaxel. miRNAs were incorporated into DOPC nanoliposomes and administered twice a week for 5 weeks via tail vein injections. CTL miRNA-treated mice had markedly larger tumor compared to the tr.

eatment groups (Fig. 4a). We found a significant difference between the paclitaxel combination groups (paclitaxel + miR-1246 inhibitor vs paclitaxel + CTL miRNA inhibitor) in tumor weight (Fig. 4a). Although there was a decreasing pattern in number of nodules in mice treated with CTL miRNA inhibitor vs miR-1246 inhibitor, the difference was not statistically significant (Fig. 4b). There was no significant difference in body weight, indicating no evidence of treatment-related toxicity ($p > 0.05$, Fig. 4c).

Given the in vitro effects of miR-1246 mimic treatment on proliferation ability of OC cells, we performed Ki67 staining to examine the biological effects of miR-1246 inhibition on tumor cell proliferation in vivo. Paraffin-embedded resected tumors were stained for Ki67 antibody. Mice treated with miR-1246 inhibitor showed significant reduction in cell proliferation compared with CTL miRNA ($p < 0.05$, t-test, Fig. 4d). Furthermore, consistent with our in vitro data, combination therapy with miR-1246 inhibitor resulted in a significantly lower number of Ki67-positive cells compared with combination of paclitaxel with CTL miRNA ($p < 0.05$, t-test, Fig. 4d). These data demonstrated that miR-1246 inhibitor treatment alone or in combination with paclitaxel was significantly associated with decreased OC cell proliferation. Next, we stained the tumors for Cav1 and PDGFRβ expression. We found that mice treated with miR-1246 inhibitor had higher Cav1 expression compared to the CTL miRNA inhibitor group (Fig. 4e). Moreover, we found that mice treated with miR-1246 inhibitor had lower PDGFRβ expression compared to the CTL miRNA inhibitor group (Fig. 4f).

2.4. miR-1246 confers paclitaxel resistance in OC cells through Cav1 and p-gp interaction

On the basis of our in vivo findings, we also investigated whether miR-1246 inhibitor treatment would be effective in the inhibition of OC cell survival in vitro. We performed the colony formation assay to evaluate OC cell proliferation upon miR-1246 inhibitor treatment alone as well as in combination with paclitaxel. Although we did not find any significant changes between the miR-1246 inhibitor alone and CTL miRNA inhibitor groups for HeyA8 or SKOV3ip1, we observed a substantial decrease in cell proliferation for paclitaxel (1 nM) plus miR-1246 inhibitor compared to paclitaxel plus CTL miRNA inhibitor (Fig. 5a). This finding indicated that miR-1246 inhibition enhanced paclitaxel effects on OC cells.

To further evaluate the role of Cav1 in drug resistance mechanisms, we examined the levels of Cav1 as well as multidrug resistance protein 1 (also called p-gp, MDR1 or ABCB1) levels which is a protein highly expressed in resistant OC cell lines (HeyA8-MDR, SKOV3-TR). We found opposite expression patterns for Cav1 and p-gp proteins in resistant vs sensitive cells by western blot experiments (Fig. 5b). To address whether p-gp expression effected by the alteration in Cav1 protein levels, we performed expression rescue experiments using a Cav1 lentiviral vector to overexpress Cav1 protein in MDR and TR resistant cell lines. Overexpression of Cav1 in MDR and TR OC cells was shown by western blot (Fig. 5c). When we overexpressed Cav1, pgp protein levels were substantially decreased in both resistant cell lines (Fig. 5c).

Next, we determined IC_{50} values for paclitaxel in CTL lentiviral- and Cav1 lentiviral-transfected MDR cell lines. We found 5 μM paclitaxel concentration as the IC_{50} value for Cav1 lentiviral-transfected cells, whereas CTL lentiviral-transfected cells did not reach IC_{50} even at 50 μM (Fig. 5d). Next, we performed time-response experiments with CTL and Cav1 lentiviral-transfected MDR cell lines using 5 μM paclitaxel

treatment. There was a significant decrease in cell proliferation for Cav1 lentiviral-transfected cells compared to CTL lentiviral-transfected cells at the 48 and 72 h time points (Fig. 5e). Then, we performed a cell viability assay using CTL miRNA and miR-1246 inhibitor miRNA-transfected MDR cell lines using varying doses of paclitaxel to show that miR-1246 is involved in drug resistance mechanisms. The miR-1246 inhibitor-treated cells had significantly lower viability compared to CTL miRNA-treated cells at 1, 5, 25 and 50 μM paclitaxel concentrations (Fig. 5f).

2.5. Exosomal miR-1246 mediates oncogenic behavior in the tumor microenvironment

Next, we addressed whether there is a difference between control and miR-1246 mimic treated mice in terms of number of macrophages recruited to the tumor site. To this end, F4/80 macrophage marker was used to evaluate macrophage levels upon treatment of mice with miR-1246 inhibitor alone or in combination with paclitaxel (Fig. 6a). We observed a reduced number of macrophages recruited by tumors in miR-1246 inhibitor-treated than in CTL inhibitor-treated mice ($p < 0.05$, t-test). The combination of paclitaxel with miR-1246 inhibitor resulted in even fewer macrophages compared to the CTL miRNA–paclitaxel combination ($p < 0.05$, t-test).

To further elucidate the role of exosomal miR-1246 in tumor macrophages, we checked the level of Cav1 protein in M0, M1 and M2 macrophages as well as in undifferentiated macrophage cells (THP-1) (Fig. 6b). Cav1 levels were found to be expressed at the lowest level in M2-type tumor-associated macrophages. Interestingly, we found that p-gp (MDR1) protein had higher expression in M2 macrophages than in M0, M1 and undifferentiated macrophage cells. These results suggest that M2-type tumor-associated macrophages may play an important role in drug-resistant mechanisms in the tumor microenvironment.

To determine whether exosomal miR-1246 released from OC cells can be taken up by cells in the tumor microenvironment, M2 macrophages were co-cultured with SKOV3-ip1 OC cells. Then, we isolated RNAs from M2-type macrophages and checked the levels of miR-1246 and its target protein Cav1. qPCR experiments revealed that co-culturing M2 macrophages with SKOV3-ip1 OC cells resulted in significantly higher miR-1246 levels compared to the levels in M2 macrophages cultured alone (Fig. 6c). This result indicates that OC cells can transfer their miRNAs to the cells present in the tumor microenvironment. Moreover, we also found significantly lower levels of Cav1 in M2-type macrophages co-cultured with OC cells than in M2 macrophages cultured alone (Fig. 6d).

To further delineate whether the inhibitory effect on target protein was coming from exosomal miRNAs, we treated the M2-type macrophage cells with exosomes isolated from SKOV3-ip1 cells and from SKOV3-ip1 cells that were pre-treated with GW4869 exosome inhibitor (SKOV3-ip1GW4869). M2-type macrophages had significantly lower Cav1 mRNA levels in the group treated with exosomes from SKOV3-ip1 than in the no-treatment group (Fig. 6e). In addition, the group treated with exosomes from SKOV3-ip1GW4869 cells did not show any significant change in Cav1 mRNA levels when compared to the no-treatment group. These results shows that oncogenic genetic materials released via OC exosomes exhibit their oncogenic action in the tumor microenvironment via tumor-associated macrophages (Fig. 7).

3. Discussion

The major finding of our study is that oncogenic miR-1246 is present and abundant in primary tumor, and OC cells and their microenvironment via their exosomes when compared to healthy controls or normal ovarian cells and exosomes. Overexpression of Cav1, the direct target of miR-1246, significantly sensitized OC cells to paclitaxel, which is evident by the decreased p-gp (MDR1) protein levels. When we block
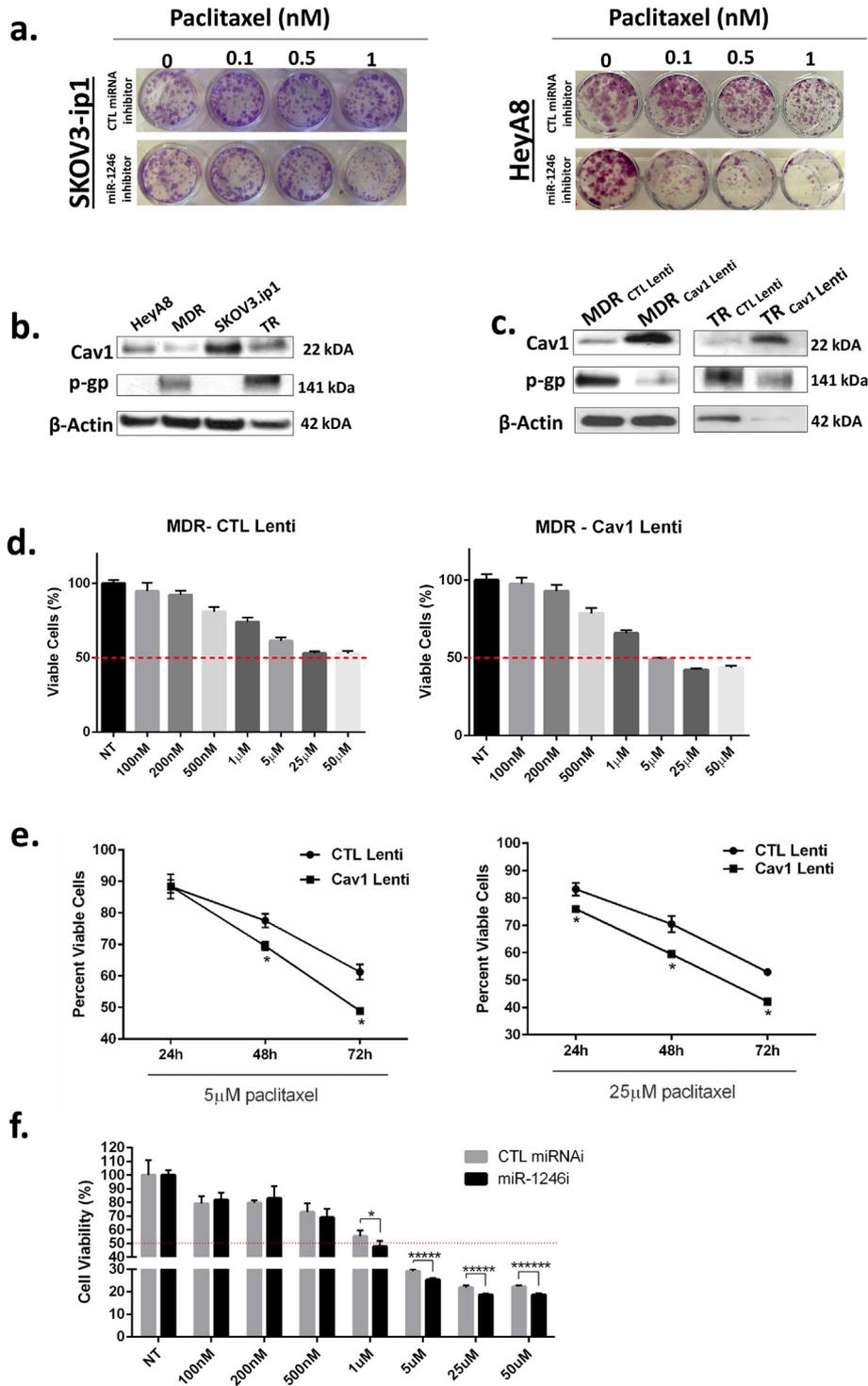
Fig. 5. miR-1246 plays a role in chemosensitization in OC cells via Cav1. a. Effect of miR-1246 inhibitor treatment in combination with varying doses of paclitaxel on cell proliferation of HeyA8 (top) and SKOV3-ip1 (bottom) cells was shown by colony formation assay. b. Western blotting of OC cell line panel for Cav1 and p-gp (MDR1) protein levels. Cav1 and p-gp had opposite expression patterns. β-actin was used as a housekeeping protein. c. MDR and TR resistant OC cells were transfected with Cav1 lentivirus. Increased expression of Cav1 was shown by western blotting. P-gp levels were decreased in Cav1 lentiviral-transfected cells. d. MTS cell viability assay was performed on either CTL or Cav1 lentiviral-transfected MDR cells treated with varying paclitaxel concentrations. IC_{50} of Cav1 lentiviral-transfected cells was found to be 5 μM, whereas CTL lentiviral-transfected cells had an IC_{50} value of >50 μM for paclitaxel at 72 h. e. Time response MTS cell viability experiment using 5 μM (left) and 25 μM (right) paclitaxel in MDR cells transfected with either CTL or Cav1 lentivirus. f. MTS cell viability experiments after treating MDR cells with either CTL or miR-1246 inhibitor for varying concentrations of paclitaxel.

the direct targeting of Cav-1 by miR-1246 via anti-miR treatment and use it in combination with paclitaxel, we showed that the treatment significantly reduced tumor growth in vitro as well as tumor burden in an orthotopic SKOV3-ip1 OC mouse model. In addition, circulating immune cells have high levels of miR-1246, and the level of miR-1246 was increased in M2-type macrophages, but not M0-type macrophages,

upon co-culturing with OC cells. Our results indicate that oncogenic miR-1246 plays an important role in chemo-resistance via inhibition of Cav1 and that exosomal miR-1246 promotes tumor progression in the tumor microenvironment via M2-type oncogenic macrophages. Furthermore, miR-1246 inhibitor treatment resulted in decreased PDGFRβ and ki67 levels in in vivo model. These results elucidate a
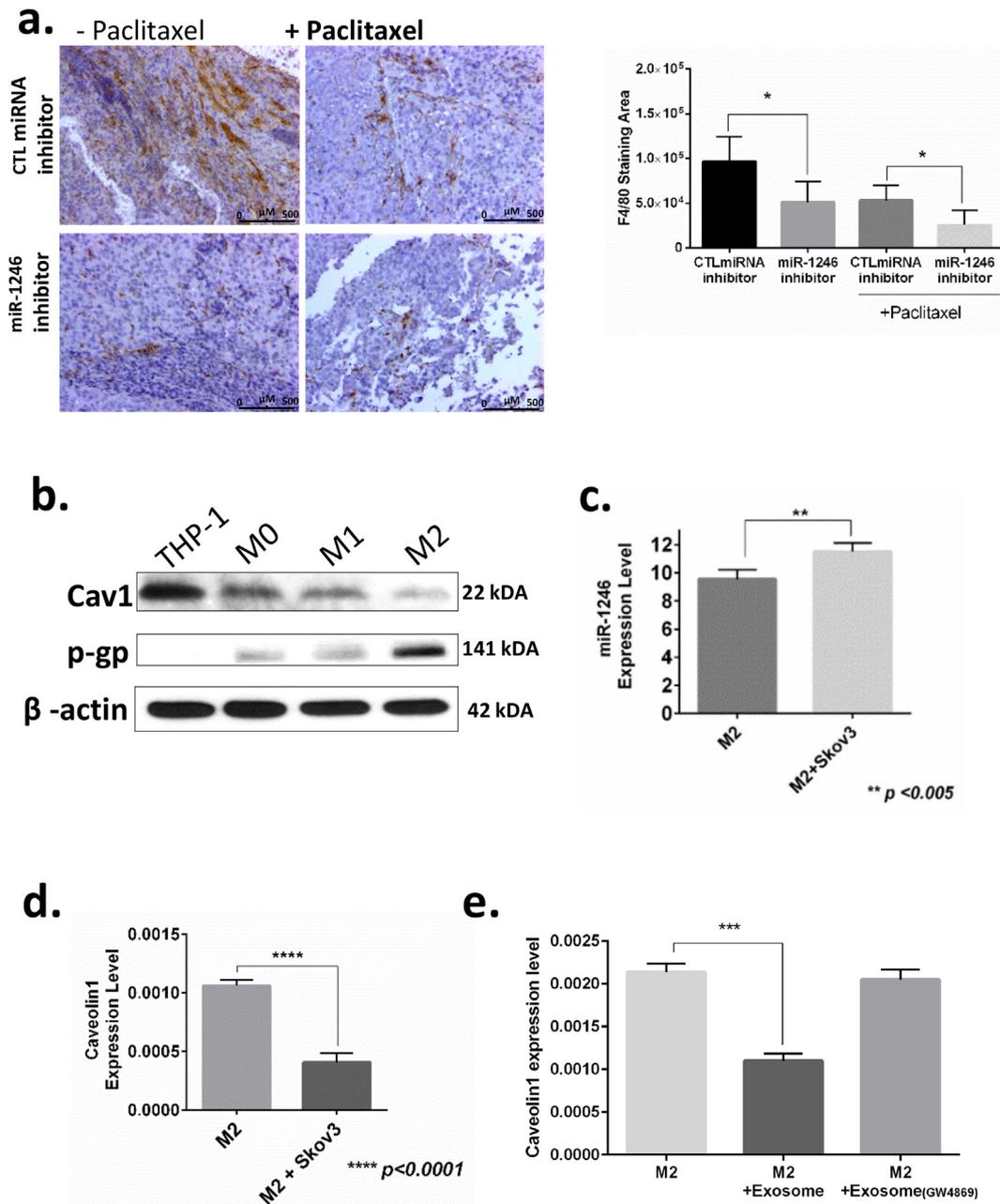
Fig. 6. Uptake of oncogenic miR-1246 by tumor-associated macrophages in the tumor microenviroment. a. F4/80 macrophage marker was used to evaluate the macrophage levels upon treatment with miR-1246 inhibitor or CTL miRNA inhibitor alone or in combination with paclitaxel in an in vivo model. b. Levels of Cav1 and p-gp levels were detected in THP-1, differentiated THP-1 (M0), M1 and M2 type macrophages by western blotting. c. qPCR analysis of miR-1246 in M2-type macrophages cultured with or without SKOV3-ip1 OC cells. d. qPCR analysis of Cav1 in M2-type macrophages cultured with or without SKOV3-ip1 OC cells. e. qPCR analysis of Cav1 in M2-type macrophages alone, M2-type macrophages treated with exosomes isolated from SKOV3-ip1 OC cells and M2-type macrophages treated with exosomes isolated from SKOV3-ip1 cells that were pretreated with GW4869 exosome inhibitor. $^*p < 0.05$, $^{**}p < 0.01$, $^{***}p < 0.001$, $^{****}p < 0.0001$ (t-test), data are presented as mean $\pm$ SD.

new mechanism for overcoming chemoresistance and tumor progression in OC cells.

During tumor progression, changes associated with oncogenic behavior ultimately affect the regulation of gene expression in primary tumors as well as metastatic sites. Expression of many miRNAs are often dysregulated in cancer. The expression of miR-1246 has been shown to be significantly upregulated in both primary tumors as well as patient serum in varied cancers such as oral squamous cell carcinoma and colorectal, breast and colon [20,31–33]. The high expression of miR-1246 has also been shown to be associated with poor patient survival in many cancers [20,24]. In OC, miR-1246 levels were shown to be elevated in serum samples from high-grade serous OC (HGSOC) patients [34]. Here, our results indicates that miR-1246 levels are significantly

higher in primary tumors from HGSOC patients compared to healthy controls. In order to have robust conclusions on cell culture studies, we used commercially available exosome depleted fetal bovine serum to certainly avoid detection of miR-1246 coming from fetal bovine serum exosomes. Our results showed that exosomes isolated from six different OC cell lines had significantly higher levels of miR-1246 compared to normal OC cells ($p < 0.05$, t-test). Overall, miR-1246 is highly expressed in both the primary tumor and patient serum in ovarian cancer.

Tumor-associated macrophages are considered an important part of the tumor microenvironment [35]. Infiltration of tumor-associated macrophages in tumor sites correlates with poor patient survival [36]. Exosomes have been shown to modulate cellular communication via
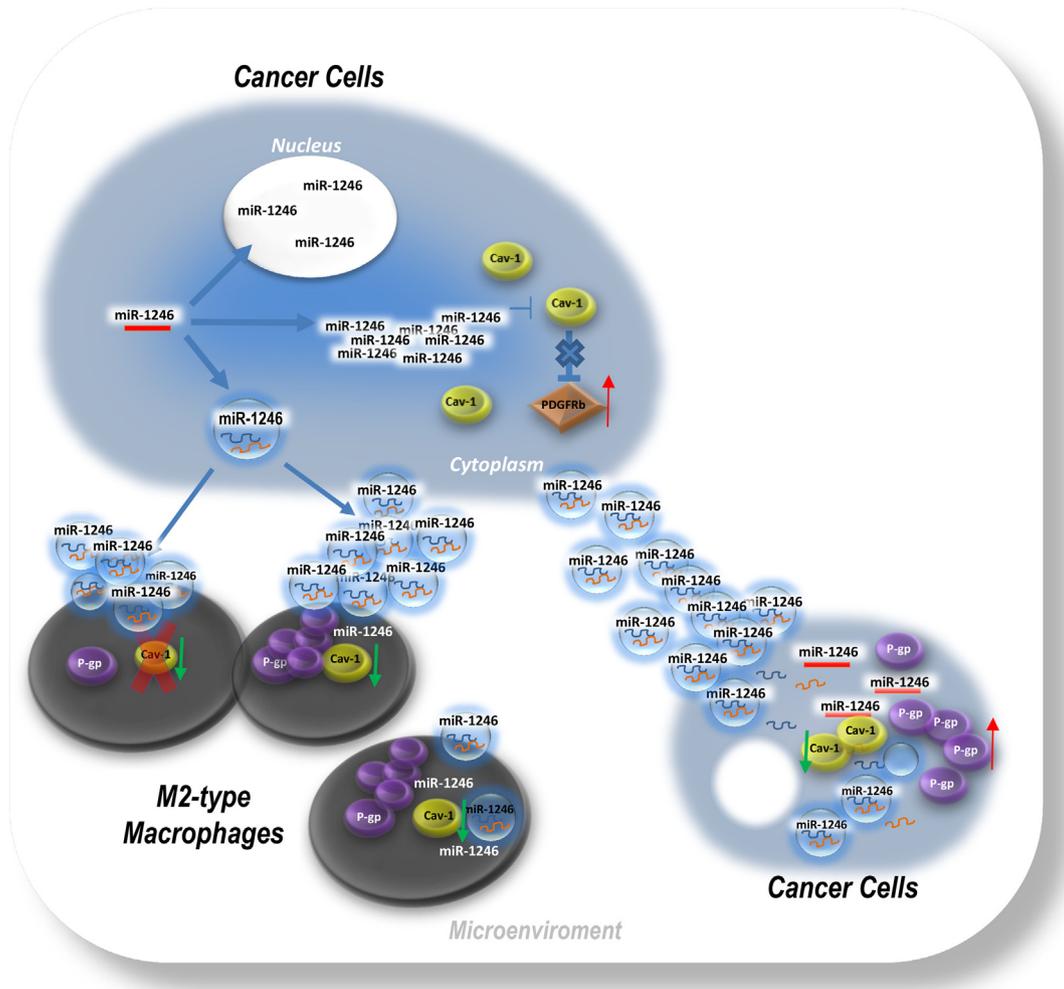
Fig. 7. miR-1246 promotes oncogenic activity in ovarian cancer cell as well as in the tumor microenvironment. Mechanistic picture showing that miR-1246 directly targets Cav1 in OC cells. Cav1 inhibition leads to increased levels of PDGFRβ protein. Exosomal miR-1246 in the tumor microenvironment is taken up by tumor-associated immune cells.

macrophages. Pancreatic cancer cells were shown to be capable of reprogramming M1-type pro-inflammatory macrophages to M2-type pro-tumorigenic macrophages via their exosomal miRNAs [37]. In this latter study, authors showed that cells transfected with miR-155 and miR-125b-2 expressing plasmid DNA release exosomes enriched in these miRNAs, which resulted in reprogramming of the macrophages to M1 phenotype. There is a recent study showing a non-cell-autonomous mechanism in which tumor cells bearing mutant p53 reprogram macrophages to an oncogenic and anti-inflammatory phase through exosomal miR-1246. Here, we showed that when OC cells are co-cultured with macrophages, they are capable of transferring their oncogenic miR-1246 selectively to M2-type macrophages, but not M0-type macrophages. In order to show selective inhibition, we blocked exosome release using GW4869 which is a specific inhibitor for natural sphingomyelinase (nSMases) and has been confirmed to abrogate exosome release [35,38]. However, two isoforms (nSMase2 and 3) have different contributions to the biogenesis of exosomes and GW4869 has been shown to lead decreased exosome release, but increased secretion of multivesicular bodies from the plasma membrane [39].

It has also been previously shown that overexpression of caveolin-1 sensitize doxorubicin resistant breast cancer cells by inhibiting P-glycoprotein transport activity [40]. The introduction of K176R mutation on Cav1 led to increased p-gp transport activity in Cav1 overexpressing non-small-cell lung cancer cells [41]. The inverse correlation between Cav1 and p-gp protein levels in ovarian cancer cells may result in enhanced chemo-sensitivity by the inhibition of p-gp protein levels

or the activity by Cav1 overexpression. Our combination therapy of miR-1246 inhibitor with paclitaxel also resulted in a substantial decrease in the proliferation of OC cells compared to that treated with CTL inhibitor. Thus, Cav1 may mediate paclitaxel sensitization in OC via regulating the expression of p-gp in OC cells.

Several studies have shown that macrophages mediate chemo resistance by modifying the expression of survival factors and/or active form of anti-apoptotic programs in malignant cells [42]. A recent study demonstrated that miR- 155-5p/C/EBPb/IL6 signaling in TAMs could stimulate chemoresistance of colorectal cancer cells by organizing the IL6R/STAT3/miR-204-5p pathway in colorectal cancer microenvironment [43]. In ovarian cancer, tumor progression and clinical outcome are negatively associated with increased macrophage density [42]. In addition, the specific surface markers existing on TAMs and cytokines that are crucial in TAM function are also raised in human ovarian cancers and linked with diminished survival [35]. Similarly, we showed that exosomal miR1246 causes paclitaxel resistance by regulating the Cav-1/p-gp/M2 axis. Recent studies have shown that exosomes are also mediators of acquired drug resistance in many cancers via their contents such as miRNAs and mRNAs [6,44–46]. We demonstrated selective dysregulation of Cav1 levels in macrophages when they are co-cultured with SKOV3-ip1 OC cells. Therefore, substantial release of miR-1246 to the tumor microenvironment via exosomes may contribute to increased drug resistance in OC patients and targeting chemoresistance through miR-1246 inhibitors offers great therapeutic potential.

Targeting PDGFRβ signaling via small molecule inhibitors has been used in cancer treatment in clinical settings since over activity of PDGFR signaling has been associated with increased tumor growth [47,48]. PDGF produced by immune cells such as macrophages contributes to increased interstitial fluid pressure in tumors, which brings about major limitations to chemotherapy treatment of these tumors because of reduced drug transport and uptake [49]. We found that high expression of PDGFRβ receptor is significantly ($p < 0.05$, long-rank test) associated with poor disease-free survival in OC patients. In our in vivo animal model, we demonstrated that miR-1246 inhibitor in combination with paclitaxel treatment significantly (p < 0.05, t-test) reduced PDGFR levels and resulted in reduced tumor burden and decreased tumor cell proliferation. Reduced PDGFRβ levels and increased Cav1 expression upon miR-1246 inhibitor treatment may improve the uptake and transport of paclitaxel by inhibiting pgp activity in OC patients.

In conclusion, we demonstrated that miR-1246 is released in abundance from OC cells and is taken up by infiltrating pro-tumorigenic cells present in the tumor microenvironment, suggesting that the tumor microenvironment plays a favorable role in tumor progression through the help of cancer exosomes. The negative correlation between Cav1 and p-gp proteins indicates the role of Cav1 in paclitaxel sensitization through reduced pgp protein levels; thus, using miR-1246 inhibitor in combination with paclitaxel provides a dual strong therapeutic approach to chemosensitization and antitumor therapy for OC patients.

4. Materials and methods

4.1. Cell culture and clinical tissue specimens

Human OC cell lines HeyA8, SKOV3-ip1, A2780, HeyA8-MDR, SKOV3-TR, A2780-CP20 and THP-1 and immortalized normal ovarian epithelial cell line HIO180 were cultured in RPMI1640 medium (Gibco BRL, Rockville, MD) supplemented with 10% fetal bovine serum (FBS) and 1% penicillin/streptomycin solution. Macrophage polarization was obtained by culturing cells in RPMI-1640 medium treated with PMA (for M0 polarization) and culturing an additional 72 h after the addition of IL-4 and IL-13 for M2 polarization. All cells were cultured at 37 °C with 5% CO_2 and 95% air and tested for mycoplasma using a mycoplasma detection kit (Lonza, Rockland, ME) as described by the manufacturer.

OC tissue samples ($n = 15$) and normal ovarian surface epithelium specimens ($n = 7$) were obtained from patients who underwent surgery at MD Anderson and Saitama Medical University (Saitama, Japan). Normal samples were normal fallopian tube epithelium or normal ovarian surface epithelium. All patients signed consent in accordance with the guidelines of the M.D. Anderson Cancer Center Institutional Review Board.

4.2. Isolation of exosomes and measurement of exosomes by nanoparticle tracking

Total exosome isolation reagent (Invitrogen) was used to isolate OC cells (HeyA8, HeyA8-MDR, SKOV3-ip1, SKOV3-TR, A2780, A2780-CP20), and cells were expanded in tissue culture plates. After cell cultures reached 70% confluency, cells were washed with PBS and incubated with 10% bovine exosome-depleted FBS (System Biosciences and/or Gibco) for 24 h. All cell culture media were collected in tubes and centrifuged at 2000 x g for 30 min, and the supernatant was filtered through a 0.22-mm PVDF filter (Millipore, Billerica, MA). An appropriate half volume of total exosome isolation reagent (Invitrogen) was added to the filtered culture medium and incubated at 4 °C overnight. The samples were centrifuged at 10,000 x g at 4 °C for 1 h, and the exosome pellets were suspended in 150 μL PBS. Exosomes were then ready for RNA extraction or exosome quantification. Exosomes were diluted in PBS (1:100) and measured using a NanoSight instrument (Malvern,

London, UK). Three replicate histograms for each sample were generated using the NanoSight instrument.

4.3. In situ hybridization

The formalin-fixed, paraffin-embedded tissue sections were dewaxed in xylene and rehydrated through an ethanol dilution series. Tissue sections were digested with 15 μg/mL proteinase K for 10 min at room temperature and were then loaded onto a Ventana Discovery Ultra system for in situ hybridization analysis. The tissue slides were hybridized with the double-DIG labeled miRCURY LNA microRNA probe (Exiqon) for 2 h at 50 °C (Ventana Discovery Ultra). The digoxigenins can then be detected with a polyclonal anti-DIG antibody and alkaline phosphatase-conjugated secondary antibody (Ventana) using NBT-BCIP as the substrate.

4.4. miRNA transfection

SKOV3 and HeyA8 cells were seeded at 4×10^4 cells/mL in 6-well plates and transfected at 50–60% confluence with miR-1246 mimic (50 nM, Life Technologies), miR-1246 inhibitor (50 nM, Life Technologies) or with a mimic/inhibitor CTL (50 nM, Life Technologies) using HiPerFect transfection reagent (Qiagen). After transfection, cells were incubated in complete medium for 72 h and processed for each experiment.

4.5. Cell extracts and western blot analysis

Total cell extracts were prepared in standard RIPA buffer with protease inhibitor cocktail and phosphate inhibitor (Roche, Basel, Switzerland). Lysates were centrifuged at 13,000 ×g for 15 min at 4 °C, and supernatants were collected. The protein concentration of cells was determined using Pierce BCA protein assay kit (Thermo Scientific). Samples were boiled at 100 °C for 5 min, separated on SDS polyacrylamide with a 4% to 15% gradient gel and transferred to polyvinylidene difluoride (PVDF) membranes. The expression levels of selected proteins were detected by using primary antibodies for Cav1, PDGFR β, p27, Rb and Notch3 (Cell Signaling, USA). The blots were then incubated with HRP-conjugated secondary antibodies. Immunoblots were developed using HyGLO Chemiluminescent HRP Antibody Detection Reagent (Denville Scientific), and signals were recorded using X-ray film. β-Actin served as an internal control. The blots were quantified by densitometry relative to β-actin.

4.6. RNA extraction, reverse transcription and quantitative real-time PCR analysis

Total RNA was extracted from cultured cells, patient tissue and exosomes by TRIzol (Invitrogen) according to the manufacturer instructions. Nuclear and cytoplasmic RNA was isolated from OC cells using the PARIS kit (Thermo Fisher, Waltham, MA).

For the miR-1246 expression analysis, 1 μg of total RNA was transcribed to complementary DNA by qScript microRNA cDNA Synthesis Kit (Quanta BioSciences) under the following conditions: 37 °C for 60 min, 70 °C for 5 min, 42 °C for 20 min and 85 °C for 5 min. All real-time PCR reactions were performed using a CFX 384 Real Time PCR System (Biorad, Hercules,CA) using the PerfeCTa microRNA Assay Kit. All primers were purchased from Quanta BioSciences. miRNA data were normalized to the internal control small nuclear RNA RNU6B, and miR-1246 expression levels were determined using the 2–ΔCT method.

4.7. RPPA analysis

RPPA microarrays were performed as described previously [28]. After miR-1246 mimic or CTL transfection, cells were washed with PBS. Lysis buffer with protease/phosphatase inhibitors was added to

stabilize phosphorylation. Cell lysates were centrifuged at 14,000 rpm for 10 min at 4 °C.The protein content of lysates was first determined using a Pierce BCA protein assay kit (Thermo Scientific). Protein samples were adjusted to 1.0 μg/μL. Protein samples were denatured at 100 °C for 5 min and stored at −80 °C until RPPA processing.

4.8. Luciferase reporter assay

The 3′ untranslated region (3′ UTR) reporter construct of the Cav1 gene was purchased from Genecopoeia. HeyA8 and SKOV3 cells (1 × 10³) were seeded in 96-well plates 1 day before transfection. Then, HeyA8 and SKOV3 cells were cotransfected with the Cav1 3′-UTR reporter vector (0.5 μg/well) and miR-1246 mimics or CTL miRNA (50 nM) by the use of HiperFect transfection reagent (Qiagen). After 48 h, firefly and Renilla luciferase activities were measured using the Luc-Pair miR Luciferase Assay according to the manufacturer's instructions (Genecopoeia). Relative luciferase activity was normalized with Renilla luciferase activity.

4.9. Animal studies and immunohistochemistry

SKOV3 cells were injected intraperitoneally in female athymic nude mice at the age of 6 weeks (1 × 10⁶ cells/mouse) to generate tumors. A total of 40 nude mice were divided into 4 groups randomly (CTL inhibitor, miR-1246 inhibitor, CTL inhibitor + paclitaxel and miR-1246 inhibitor + paclitaxel). For in vivo delivery, miR-1246 mimic and CTL inhibitor (Life Technologies) were incorporated into liposomes. After 1 week, mice were treated with liposomal nanoparticles containing miR-1246 inhibitor or CTL inhibitor (200 μg/kg/mouse) twice weekly. Also, paclitaxel (100 μg/100 μL) was intraperitoneally injected in the mice. After completion of treatment, mice were killed to measure tumor growth. Tumor tissues were collected and analyzed by immunohistochemistry analysis. All animal work was approved by the Institutional Animal Use and Care Committee of MD Anderson.

The immunohistochemical analysis was performed using paraffin-embedded mouse tissues. First, unstained sections were deparaffinized and rehydrated. Following antigen retrieval with DAKO antigen retrieval solution (DAKO, North America Inc., Carpinteria, CA), endogenous peroxidase was blocked using 3% hydrogen peroxide. After blocking for 20 min, primary antibodies against Ki67, Cav1 and PDGFRβ were incubated overnight at 4 °C. The next day, they were incubated with the appropriate secondary antibody for 1 h at room temperature. Slides were developed with DAB substrate (Vector Labs) and counterstained with hematoxylin solution and then quantified. For Cav1 and PDGFRβ staining, images were taken at 20× magnification and quantified with the ImageJ software (http://rsb.info.nih.gov/ij/) by performing colour deconvolution based on 3,3′-diaminobenzidine (DAB) staining [50]. For Ki67 index, positive cells were counted in five random fields per slide.

4.10. Survival analysis

TCGA mRNA microarray (Agilent 244 K Custom Gene Expression G4502A-07, Affymetrix Human Genome U133A 2.0 Array, Affymetrix Human Exon 1.0 ST Array) and RNASeqv2 level 3 data for patients with ovarian carcinoma were retrieved from Broad GDAC Firehose (http://gdac.broadinstitute.org/). Clinical information for these patients was obtained from cBioPortal (http://www.cbioportal.org/). Survival analysis was performed in R (version 3.2.5). The relationship between overall survival, disease-free survival and covariates (mRNA expression levels and clinical parameters [age and stage]) was examined using a Cox proportional hazard model. A multivariate Cox proportional hazard model was fitted, including the clinical parameters and mRNA expression significant in the univariate analysis. For PDGFRβ, patients were divided into tertiles according to PDGFRβ mRNA expression, and the first and last tertiles were contrasted. For Affymetrix Human Exon 1.0 ST

Array data, PDGFRB was an independent prognostic factor for poor disease-free survival. The Kaplan-Meier method was used to generate survival curves. For each group (those with high vs low PDGFR1 expression), median disease-free survival in months as well as number of patients at risk at different time points were plotted. For overall survival analysis of Cav1, samples ($n = 482$) from TCGA were grouped into high (top quartile) expression level versus low (all other samples) expression. Also, samples with detectable miR-1246 ($n = 138$) were divided into high ($n = 69$) versus low (n = 69) groups according to Cav1 (cut-off, median expression was 7.05) and miR-1246 (cut-off, median expression was 0.029) median expression and overall survival curves were generated by Kaplan-Meier method. Additionally, the cohort was split into 4 groups by setting Cav1 and miR-1246 cutoff levels corresponding to low/high mRNA and low/high miRNA expression: low/low, low/high, high/low, and high/high and overall survival curves was plotted between the low Cav1/high miR-1246 and high Cav1/low miR-1246 subsets of patients.

4.11. Statistical analysis

Quantitative data were compared by the Student t-test for different treatment groups, and p-values <0.05 were considered significant. The Shapiro-Wilk test was used to test the normality of the distribution of the data. Quantitative data are presented as the means ± SD of three independent experiments.

To quantify differences in gene expression level of Cav1 in normal ovary versus ovarian tumor samples, four independent datasets (GSE18271, GSE27651, GSE38666 and GSE40595) were analyzed by using a t-test and p-values < 0.05 were considered significant.

Appendix A. Supplementary data

Supplementary data to this article can be found online at https://doi.org/10.1016/j.ebiom.2018.11.004.

References

[1] Wang Z, Chen JQ, Liu JL, Tian L. Exosomes in tumor microenvironment: novel transporters and biomarkers. J Transl Med 2016;14.

[2] Song J, Chen X, Wang M, Xing Y, Zheng Z, Hu S. Cardiac endothelial cell-derived exosomes induce specific regulatory B cells. Sci Rep 2014;4:7583.

[3] Azmi AS, Bao B, Sarkar FH. Exosomes in cancer development, metastasis, and drug resistance: a comprehensive review. Cancer Metastasis Rev 2013;32(3–4):623–42.

[4] McDonald MK, Tian YZ, Qureshi RA, Gormley M, Ertel A, Gao R, et al. Functional significance of macrophage-derived exosomes in inflammation and pain. Pain 2014; 155(8):1527–39.

[5] Viaud S, Terme M, Flament C, Taieb J, Andre F, Novault S, et al. Dendritic Cell-Derived Exosomes Promote Natural Killer Cell Activation and Proliferation: a Role for NKG2D Ligands and IL-15R alpha. PLoS One 2009;4(3).

[6] Chen WX, Liu XM, Lv MM, Chen L, Zhao JH, Zhong SL, et al. Exosomes from drug-resistant breast cancer cells transmit chemoresistance by a horizontal transfer of microRNAs. Plos One 2014;9(4).

[7] Syn N, Wang LZ, Sethi G, Thiery JP, Goh BC. Exosome-mediated metastasis: from epithelial-mesenchymal transition to escape from immunosurveillance. Trends Pharmacol Sci 2016;37(7):606–17.

[8] Ye SB, Li ZL, Luo DH, Huang BJ, Chen YS, Zhang XS, et al. Tumor-derived exosomes promote tumor progression and T-cell dysfunction through the regulation of enriched exosomal microRNAs in human nasopharyngeal carcinoma. Oncotarget 2014;5(14):5439–52.

[9] Costa-Silva B, Aiello NM, Ocean AJ, Singh S, Zhang HY, Thakur BK, et al. Pancreatic cancer exosomes initiate pre-metastatic niche formation in the liver. Nat Cell Biol 2015;17(6):816.

[10] Hoshino A, Costa-Silva B, Shen TL, Rodrigues G, Hashimoto A, Mark MT, et al. Tumour exosome integrins determine organotropic metastasis. Nature 2015;527 (7578):329.

[11] Falcone G, Felsani A, D'Agnano I. Signaling by exosomal microRNAs in cancer. J Exp Clin Cancer Res 2015;34.

[12] Yu Z, Li Y, Fan H, Liu Z, Pestell RG. miRNAs regulate stem cell self-renewal and differentiation. Front Genet 2012;3:191.

[13] Hartig SM, Hamilton MP, Bader DA, McGuire SE. The miRNA interactome in metabolic homeostasis. Trends Endocrinol Metab 2015;26(12):733–45.

[14] Jeker LT, Bluestone JA. MicroRNA regulation of T-cell differentiation and function. Immunol Rev 2013;253:65–81.

[15] Inui M, Martello G, Piccolo S. MicroRNA control of signal transduction. Nat Rev Mol Cell Biol 2010;11(4):252–63.

[16] Bayraktar R, Pichler M, Kanlikilicer P, Ivan C, Bayraktar E, Kahraman N, et al. MicroRNA 603 acts as a tumor suppressor and inhibits triplenegative breast cancer tumorigenesis by targeting elongation factor 2 kinase. Oncotarget 2017;8(7): 11641–58.

[17] Chen X, Ba Y, Ma LJ, Cai X, Yin Y, Wang KH, et al. Characterization of microRNAs in serum: a novel class of biomarkers for diagnosis of cancer and other diseases. Cell Res 2008;18(10):997–1006.

[18] Ogata-Kawata H, Izumiya M, Kurioka D, Honma Y, Yamada Y, Furuta K, et al. Circulating Exosomal microRNAs as Biomarkers of Colon Cancer. Plos One 2014;9 (4).

[19] Mar-Aguilar F, Mendoza-Ramirez JA, Malagon-Santiago I, Espino-Silva PK, Santuario-Facio SK, Ruiz-Flores P, et al. Serum circulating microRNA profiling for identification of potential breast cancer biomarkers. Dis Markers 2013;34(3):163–9.

[20] Takeshita N, Hoshino I, Mori M, Akutsu Y, Hanari N, Yoneyama Y, et al. Serum microRNA expression profile: miR-1246 as a novel diagnostic and prognostic biomarker for oesophageal squamous cell carcinoma. Brit J Cancer 2013;108(3): 644–52.

[21] Kuhlmann JD, Hahn S, Baraniskin A, Wimberger P, Kasimir-Bauer S. MicroRNA-1246 as a novel candidate for a blood-based biomarker in ovarian cancer patients. Cancer Res 2012;72.

[22] Nagamitsu Y, Nishi H, Sasaki T, Takaesu Y, Terauchi F, Isaka K. Profiling analysis of circulating microRNA expression in cervical cancer. Mol Clin Oncol 2016;5(1): 189–94.

[23] Shimomura A, Shiino S, Kawauchi J, Takizawa S, Sakamoto H, Matsuzaki J, et al. Novel combination of serum microRNA for detecting breast cancer in the early stage. Cancer Sci 2016;107(3):326–34.

[24] Zhang WC, Chin TM, Yang H, Nga ME, Lunny DP, Lim EKH, et al. Tumour-initiating cell-specific miR-1246 and miR-1290 expression converge to promote non-small cell lung cancer progression. Nat Commun 2016;7.

[25] Hornick NI, Huan J, Doron B, Goloviznina NA, Lapidus J, Chang BH, et al. Serum exosome microRNA as a minimally-invasive early biomarker of AML. Sci Rep-Uk 2015;5.

[26] Sun Z, Meng CT, Wang SH, Zhou N, Guan M, Bai CM, et al. MicroRNA-1246 enhances migration and invasion through CADM1 in hepatocellular carcinoma. BMC Cancer 2014;14.

[27] Chen J, Yao D, Zhao S, He C, Ding N, Li L, et al. MiR-1246 promotes SiHa cervical cancer cell proliferation, invasion, and migration through suppression of its target gene thrombospondin 2. Arch Gynecol Obstet 2014;290(4):725–32.

[28] Kanlikilicer P, Rashed MH, Bayraktar R, Mitra R, Ivan C, Aslan B, et al. Ubiquitous Release of Exosomal Tumor Suppressor miR-6126 from Ovarian Cancer Cells. Cancer Res 2016;76(24):7194–207.

[29] Rashed MH, Kanlikilicer P, Rodriguez-Aguayo C, Pichler M, Bayraktar R, Bayraktar E, et al. Exosomal miR-940 maintains SRC-mediated oncogenic activity in cancer cells: a possible role for exosomal disposal of tumor suppressor miRNAs. Oncotarget 2017; 8(12):20145–64.

[30] Yamamoto M, Toya Y, Jensen RA, Ishikawa Y. Caveolin is an inhibitor of platelet-derived growth factor receptor signaling. Exp Cell Res 1999;247(2):380–8.

[31] Liao L, Wang J, Ouyang SB, Zhang P, Wang JL, Zhang M. Expression and clinical significance of microRNA-1246 in human oral squamous cell carcinoma. Med Sci Monit 2015;21:776–81.

[32] Scarpati GDV, Calura E, Di Marino M, Romualdi C, Beltrame L, Malapelle U, et al. Analysis of differential miRNA Expression in primary tumor and stroma of colorectal cancer patients. Biomed Res Int 2014;2014:8.

[33] Hannafon BN, Trigoso YD, Calloway CL, Zhao YD, Lum DH, Welm AL, et al. Plasma exosome microRNAs are indicative of breast cancer. Breast Cancer Res 2016;18.

[34] Todeschini P, Salviato E, Paracchini L, Ferracin M, Petrillo M, Zanotti L, et al. Circulating miRNA landscape identifies miR-1246 as promising diagnostic biomarker in high-grade serous ovarian carcinoma: a validation across two independent cohorts. Cancer Lett 2017;388:320–7.

[35] Colvin E. Tumor-associated macrophages contribute to tumor progression in ovarian cancer. Front Oncol 2014;4(137).

[36] Tsutsui S, Yasuda K, Suzuki K, Tahara K, Higashi H, Era S. Macrophage infiltration and its prognostic implications in breast cancer: the relationship with VEGF expression and microvessel density. Oncol Rep 2005;14(2):425–31.

[37] Su MJ, Aldawsari H, Amiji M. Pancreatic cancer cell exosome-mediated macrophage reprogramming and the role of microRNAs 155 and 125b2 transfection using nanoparticle delivery systems. Sci Rep-Uk 2016;6.

[38] Trajkovic K. Ceramide triggers budding of exosome vesicles into multivesicular endosomes (319, 1244, 2008). Science 2008;320(5873):179.

[39] Menck K, Sonmezer C, Worst TS, Schulz M, Dihazi GH, Streit F, et al. Neutral sphingomyelinases control extracellular vesicles budding from the plasma membrane. J Extracell Vesicles 2017;6(1).

[40] Cai CX, Chen JW. Overexpression of caveolin-1 induces alteration of multidrug resistance in Hs578T breast adenocarcinoma cells. Int J Cancer 2004;111(4):522–9.

[41] Lee CY, Lai TY, Tsai MK, Ou-Yang P, Tsai CY, Wu SW, et al. The influence of a caveolin-1 mutant on the function of P-glycoprotein. Sci Rep-Uk 2016;6.

[42] Ruffell B, Coussens LM. Macrophages and Therapeutic Resistance in Cancer. Cancer Cell 2015;27(4):462–72.

[43] Yin Y, Yao SR, Hu YL, Feng YY, Li M, Bian ZH, et al. The Immune-microenvironment Confers Chemoresistance of Colorectal Cancer through Macrophage-Derived IL6. Clin Cancer Res 2017;23(23):7375–87.

[44] Wei YF, Lai XF, Yu ST, Chen SN, Ma YZ, Zhang Y, et al. Exosomal miR-221/222 enhances tamoxifen resistance in recipient ER-positive breast cancer cells. Breast Cancer Res Tr 2014;147(2):423–31.

[45] Yeung CLA, Co NN, Tsuruga T, Yeung TL, Kwan SY, Leung CS, et al. Exosomal transfer of stroma-derived miR21 confers paclitaxel resistance in ovarian cancer cells through targeting APAF1. Nat Commun 2016;7.

[46] Ciravolo V, Huber V, Ghedini GC, Venturelli E, Bianchi F, Campiglio M, et al. Potential role of HER2-overexpressing exosomes in countering trastuzumab-based therapy. J Cell Physiol 2012;227(2):658–67.

[47] Heldin CH. Targeting the PDGF signaling pathway in tumor treatment. Cell Commun Signal 2013;11.

[48] Pietras K, Sjoblom T, Rubin K, Heldin CH, Ostman A. PDGF receptors as cancer drug targets. Cancer Cell 2003;3(5):439–43.

[49] Heldin CH, Rubin K, Pietras K, Ostman A. High interstitial fluid pressure - an obstacle in cancer therapy. Nat Rev Cancer 2004;4(10):806–13.

[50] Ruifrok AC, Johnston DA. Quantification of histochemical staining by color deconvolution. Anal Quant Cytol 2001;23(4):291–9.